Journal of Experimental Botany, Vol. 67, No. 10 pp. 3137–3148, 2016
doi:10.1093/jxb/erw154 Advance Access publication 27 April 2016
This paper is available online free of all access charges (see http://jxb.oxfordjournals.org/open_access.html for further details)

RESEARCH PAPER

Improved analysis of C_4 and C_3 photosynthesis via refined *in vitro* assays of their carbon fixation biochemistry

Robert E. Sharwood[1,*], Balasaheb V. Sonawane[2], Oula Ghannoum[2] and Spencer M. Whitney[1]

[1] ARC Centre of Excellence for Translational Photosynthesis, Research School of Biology, Australian National University, Canberra ACT 2601, Australia
[2] ARC Centre of Excellence for Translational Photosynthesis, Hawkesbury Institute for the Environment, Western Sydney University, Richmond NSW 2753, Australia

* Correspondence: robert.sharwood@anu.edu.au

Received 31 January 2016; Accepted 21 March 2016

Editor: Andreas Weber, Heinrich-Heine-Universität Düsseldorf

Abstract

Plants operating C_3 and C_4 photosynthetic pathways exhibit differences in leaf anatomy and photosynthetic carbon fixation biochemistry. Fully understanding this underpinning biochemical variation is requisite to identifying solutions for improving photosynthetic efficiency and growth. Here we refine assay methods for accurately measuring the carboxylase and decarboxylase activities in C_3 and C_4 plant soluble protein. We show that differences in plant extract preparation and assay conditions are required to measure NADP-malic enzyme and phosphoenolpyruvate carboxylase (pH 8, Mg^{2+}, 22 °C) and phosphoenolpyruvate carboxykinase (pH 7, >2 mM Mn^{2+}, no Mg^{2+}) maximal activities accurately. We validate how the omission of $MgCl_2$ during leaf protein extraction, lengthy (>1 min) centrifugation times, and the use of non-pure ribulose-1,5-bisphosphate (RuBP) significantly underestimate Rubisco activation status. We show how Rubisco activation status varies with leaf ontogeny and is generally lower in mature C_4 monocot leaves (45–60% activation) relative to C_3 monocots (55–90% activation). Consistent with their >3-fold lower Rubisco contents, full Rubisco activation in soluble protein from C_4 leaves (<5 min) was faster than in C_3 plant samples (<10 min), with addition of Rubisco activase not required for full activation. We conclude that Rubisco inactivation in illuminated leaves primarily stems from RuBP binding to non-carbamylated enzyme, a state readily reversible by dilution during cellular protein extraction.

Key words: Carbamylation, carbon fixation, CO_2-concentrating mechanism, photosynthesis, Rubisco, Rubisco activase.

Introduction

Plants operating the C_3 and C_4 pathways contain differing biochemical and anatomical features that facilitate their climatic adaptation to cool-temperate and warm-tropical environments, respectively (Edwards *et al.*, 2010). The rate-limiting CO_2 fixation step common to both pathways is catalysed by the photosynthetic enzyme ribulose 1,5-bisphosphate (RuBP) carboxylase/oxygenase (Rubisco, EC 4.1.1.39). Fixation of CO_2 to RuBP by Rubisco produces two molecules of 3-phosphoglycerate (PGA) that are cycled through the photosynthetic carbon reduction (PCR) cycle to produce triose-phosphates, the building blocks of carbohydrates needed for plant growth (Raines, 2003).

Rubisco is an imperfect catalyst that is remarkably slow (completing only 2–4 cycles s^{-1} in leaves) and can fix O_2

instead of CO_2, with oxygenation of RuBP leading to the production of 2-phosphoglycolate (PGly) whose recycling back to PGA by the photorespiratory pathway spans three cellular compartments and undesirably consumes energy and releases fixed CO_2 (Bauwe *et al.*, 2010). Overcoming the catalytic limitations of Rubisco by directed changes to the enzyme or concentrating CO_2 around Rubisco to reduce the costs of photorespiration are ongoing bioengineering challenges (Parry *et al.*, 2013; Price *et al.*, 2013; Long *et al.*, 2015). Current efforts to generate or discover plant Rubisco isoforms with joint improvements in specificity for CO_2 as opposed to O_2 ($S_{c/o}$) and carboxylation efficiency (defined as the maximum carboxylation rate (k_{cat}^c) divided by the K_m for CO_2 under ambient O_2; $K_C^{21\%O2}$) have yet to yield success (Sharwood and Whitney, 2014), despite such Rubiscos existing in some non-green algae (Andrews and Whitney, 2003).

The evolution of C_4 photosynthesis ~35–40 million years ago provided a natural solution to remedy the inefficiency of Rubisco (Sage *et al.*, 2012). The anatomical separation of phosphoenolpyruvate carboxylase (PEPC) in mesophyll cells (MCs) and Rubisco in the bundle sheath cell (BSC) chloroplasts was accompanied by adaptation of biochemical CO_2-concentrating mechanisms (CCMs) (Hatch, 1987; Kanai and Edwards, 1999). The C_4 pathway involves the hydration by carbonic anhydrase of CO_2 to HCO_3^- which is combined with phosphoenolpyruvate (PEP) by phosphoenolpyruvate carboxylase (PEPC) into the 4C acid oxaloacetate (OAA) that is converted into malate or aspartate before diffusing into the BSCs where they are decarboxylated, raising the CO_2 around Rubisco >4-fold higher than ambient CO_2 (von Caemmerer, 2000; Sage, 2004). The 3C decarboxylation product, pyruvate, returns to the MCs for PEP regeneration by pyruvate phosphate dikinase (PPDK) at the cost of two ATP equivalents.

The ratio of the activity between the main carboxylases is a key determinant of the efficiency of the CCM and can be an indication of the CO_2 supply to BSCs (von Caemmerer *et al.*, 2014). On the one hand, PEPC activity is much higher than that of Rubisco (2- to 10-fold depending on plant species and environmental conditions) to enable the C_4 acid gradient to build and facilitate the diffusion of the C_4 acids into the BSCs. On the other hand, the PEPC:Rubisco ratio must be optimized to minimize CO_2 leakage from the BSCs, leading to futile cycling involving the CCM (Kromdijk *et al.*, 2008). Futile cycling of the CCM is energetically wasteful for the plant through use of ATP to regenerate PEP.

Based on the main decarboxyating enzymes, C_4 plants can be grouped into three biochemical subtypes: NADP-malic enzyme (NADP-ME), NAD-malic enzyme (NAD-ME), and phosphoenolpyruvate carboxykinase (PEPCK) (Hatch, 1987; Kanai and Edwards, 1999). In addition, there is flexibility among some NADP-ME (e.g maize, sorghum, and *Panicum antidotale*) and NAD-ME (e.g. *Cleome angustifolia*, *Bienertia sinuspersici*, and *Panicum coloratum*) species which also harbour PEPCK (Furbank, 2011; Pinto *et al.*, 2014; Koteyeva *et al.*, 2015). The significance of the dual decarboxylation pathways is not yet fully understood, but evidence suggests that PEPCK allows flexibility to the decarboxylation pathway(s) that may be dependent on environmental cues (Bellasio and Griffiths, 2014; Sharwood *et al.*, 2014). Assaying for PEPCK is often difficult because pure enzyme is required for assaying in the decarboxylase direction due to interference from other C_4 pathway enzymes (Ashton *et al.*, 1990). However, assaying for PEPCK activity in the carboxylase direction is also troublesome as PEPC can interfere with this assay, although variations in PEPCK activities can be corroborated by western blot analysis of PEPCK content (Sharwood *et al.*, 2014). Accurately determining the level of maximum PEPCK activity is requisite to determine the level of flexibility in the decarboxylation pathways that may exist.

A conserved feature of Rubisco catalysis is the required priming (activation) of each catalytic site (E) located at the interface of adjoining paired 50 kDa large subunits (L_2) that arrange as $(L_2)_4$ tetrad cores and are capped at either end with tetrads of 15 kDa small (S) subunits to form an ~520 kDa L_8S_8 complex (Andersson and Backlund, 2008). Activation proceeds via the slow and reversible binding of non-substrate CO_2 to the ε-amino group of a conserved L-subunit Lys201 producing a carbamate (EC) that is rapidly stabilized by Mg^{2+} to produce a tertiary complex (ECM) capable of RuBP binding and enolization and its subsequent carboxylation or oxygenation (Andersson, 2008). *In vivo*, the pool of inactive Rubisco comprises decarbamylated catalytic sites (E) and ECM complexes binding inhibitory sugar-phosphate molecules (ECMI) (Parry *et al.*, 2008) (Fig. 1). Examples of these inhibitors include the catalytic misfire product xylulose 1,5-bisphosphate (XuBP) and the 'nocturnal' or 'shade' inhibitor 2'-carboxy-D-arabinitol 1-phosphate (CA1P) produced under low light and darkness (Gutteridge *et al.*, 1986; Moore and Seemann, 1992; Pearce, 2006; Andralojc *et al.*, 2012). Binding of RuBP to E also leads to the production of catalytically stalled ER complexes (Laing and Christeller, 1976; Jordan and Chollet, 1983). Release of these sugar-phosphate molecules is catalysed by Rubisco activase (RCA) via ATP hydrolysis (Parry *et al.*, 2008; Mueller-Cajar *et al.*, 2014). Following their RCA-facilitated release, the rebinding of XuBP and CA1P is prevented by the enzymes XuBPase (Bracher *et al.*, 2015) and CA1Pase (Salvucci and Holbrook, 1989; Moore and Seemann, 1992). The enzyme CA1Pase is

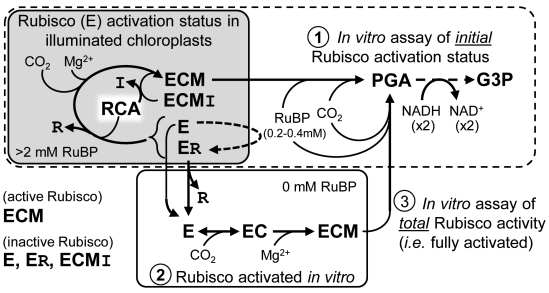

Fig. 1. Summary of Rubisco activation status *in vivo* and modulation *in vitro*. Summary of the NADH-linked assay used to determine Rubisco activation status using rapidly extracted soluble protein from young, non-stressed leaves sampled during illumination [where inactive ECMI complexes containing the Rubisco inhibitors (I) CA1P or XuBP would be negligible]. See text for details of the three assay stages indicated. R, RuBP; RCA, Rubisco activase. Details of the NADH-linked assay are summarized in Supplementary Fig. S1 and Supplementary Table S1.

also able to metabolize the inhibitor pentadiulose-1,5-bisphosphate (PDBP; Andralojc *et al.*, 2012), a relatively labile oxygenation byproduct whose inhibitory relevance *in vivo* remains indeterminate but is a significant contaminant of non-pure RuBP (Kane *et al.*, 1998). Conditions that stimulate Rubisco inactivation include increasing temperature (increased XuBP and PDBP production), low illumination (stimulated CA1P synthesis), and elevated CO_2 (possibly increases ER levels) (Crafts-Brandner and Salvucci, 2000; Salvucci and Crafts-Brandner, 2004; Kim and Portis, 2005; Parry *et al.*, 2008).

Extrapolating aspects of cellular biochemistry from leaf gas exchange measurements using available C_3 and C_4 photosynthesis models is highly reliant on accurately knowing the content and catalytic properties of the carboxylation and decarboxylation enzyme activities (Farquhar *et al.*, 1980; Salvucci and Crafts-Brandner, 2004; Sharkey *et al.*, 2007). Here we appraise and refine the methods for assaying PEPC, PEPCK, and Rubisco activity and activation status using NADH-linked spectrometric assays. We apply these refined assay methods to leaf extracts from C_3 and C_4 grasses to demonstrate their applicability in accurately measuring variations in the carboxylation/decarboxylation biochemistries of leaves of differing ontogeny.

Materials and methods

Plant seeds and growth conditions

Seeds for *Panicum bisulcatum* and *Megathyrsus maximum* were obtained from the Australian Plant Genetic Resources Information System (QLD, Australia) and Queensland Agricultural Seeds Pty. Ltd (Toowoomba, Australia), while the seeds for tobacco (*Nicotiana tabacum,* cv Petit havana), maize (*Zea mays* cv Kelvedon Glory), and wheat (*Triticum aestivum* cv Y70) were sourced locally. The seeds were sown in 2–5 litre pots of commercial self-fertilizing potting mix at 5–7 d intervals to obtain plants of different ages to sample simultaneously. The plants were grown in a glasshouse at set 28/22 °C day/night temperatures under natural illumination during November and December in Canberra, Australia. Plants were watered regularly, with the addition of Hoaglands nutrients to mature plants every 2 d.

Leaf harvesting, protein extraction, and protein assay

Samples of known area (0.3 or 0.5 cm^2) were harvested using brass cork borers (Met-App Metalware, Melbourne) from different aged leaves on the same day, 5–7 h into the light period. The samples were rapidly frozen in liquid nitrogen before storing at –80 °C. For assays of Rubisco activity and content as well as the activity of PEPC and NADP-ME, the soluble leaf protein was extracted using ice-cold 2 ml glass homogenizers (Wheaton) into 0.5–1 ml of ice cold, N_2-sparged extraction buffer [50 mM EPPS-NaOH, pH 8.0, 0.5 mM EDTA, 2 mM DTT, 1% (v/v) plant protease inhibitor cocktail (Sigma-Aldrich), and 1% (w/v) polyvinylpolypyrrolidone (PVPP)] containing 0, 2, 5, or 10 mM $MgCl_2$. The lysate was rapidly centrifuged for 0.5, 2, or 5 min (16 000 *g*, 4 °C), and 10 µl of the soluble leaf protein was assayed for initial and total Rubisco activities (see below) and 50 µl to measure Rubisco content by [^{14}C]CABP (2-C-carboxyarabinitol 1,5-bisphosphate) binding as described (Whitney *et al.*, 2001). Protein content was measured against BSA standards using a Coomassie dye binding assay (Pierce). The leaf area extracted in 1 ml of buffer was generally 0.3 cm^2 (*T. aestivum*), 0.5 cm^2 (*N. tabacum*), 0.6 cm^2 (*P. bisulcatum*), and 0.9 cm^2 (*P. bisulcatum*, *M. maximus*, and *Z. mays*)

Phosphoenolpyruvate carboxylase assay

Maximal PEPC activities were measured using an NADH-coupled assay as previously described (Ashton *et al.*, 1990). Extraction was performed using the same extraction buffer as described for Rubisco containing 5 mM $MgCl_2$, and samples were incubated at room temperature or on ice for 0, 5, 10, and 20 min before adding 10 µl of extract to initiate assays.

NADP-malic enzyme assay

Maximal NADP-ME activity was determined in a coupled NADP assay as previously described (Ashton *et al.*, 1990; Pengelly *et al.*, 2012). Briefly, NADP-ME activity in leaf extracts prepared as described above was assayed in 50 mM Tricine-KOH pH 8.3, 5 mM malic acid, initiating with 10 mM $MgCl_2$.

Phosphoenolpyruvate carboxykinase assay

The maximal activity of PEPCK was measured in the carboxylase direction using a method adapted from Chen *et al.* (2002) and Walker *et al.* (2002) as described by Sharwood *et al.* (2014) in an NADH-coupled assay as depicted in Fig. 2A. To remove interference with PEPC, $MgCl_2$ was excluded from the extraction and assay buffers. PEPC background activity was determined by assaying for PEPC activity as above with and without $MgCl_2$, with no PEPC activity observed when $MgCl_2$ is omitted from the extraction and assay buffer (data not shown). For PEPCK assay, leaf discs were extracted in 50 mM HEPES pH 7.0, 5 mM DTT, 1% (w/v) PVPP, 2 mM EDTA, 2 mM $MnCl_2$, and 0.05% Triton. PEPCK activity from leaf extracts was measured in assay buffer [50 mM HEPES, pH 7.0, 4% mercaptoethanol (w/v), 100 mM KCl, 90 mM $NaHCO_3$,1 mM ADP, 2 mM $MnCl_2$, 0.14 mM NADH, and malate dehydrogenase (MDH; 6 U; 3.7 µl)] after the addition of 15 mM PEP. An optimal PEP concentration was determined in separate assays titrated with 2.5–20 mM PEP.

Rubisco activity assays

Rubisco activity was measured at 25 °C using an NADH-coupled enzyme assay (Kubien *et al.*, 2011; Supplementary Fig. S1 at *JXB* online) with the rate of NADH oxidation monitored at 340 nm using a diode array spectrophotometer (Agilent model 8453). The RuBP used in the assays was either that synthesized and purified as previously described (Kane *et al.*, 1998) or commercially supplied (Sigma; R0878). Assays were performed in 1 ml cuvettes containing 0.48 ml of assay buffer [100 mM EPPS-NaOH, pH 8.0, 10 mM $MgCl_2$, 0.2 mM NADH, 20 mM $NaHCO_3$, 1 mM ATP, pH 7.0, 5 mM phosphocreatine, pH 7.0, and 4% (v/v) coupling enzymes] (see Supplementary Table S1). RuBP (0.4 mM) was included in the cuvettes used to measure initial Rubisco activity, with 20 µl of soluble leaf protein sample added to start the assays. To measure total Rubisco activities, 20 µl of leaf protein was first activated for 10–15 min in RuBP-free assay buffer before initiating Rubisco activity measurements by adding RuBP to 0.4 mM. The Rubisco carboxylation rate was determined using the equation:

$$\text{mol RuBP consumed}\cdot\text{min}^{-1} = \left(\frac{\Delta OD_{340}}{4\left(6.22\times10^{-3}\,\text{M}^{-1}\right)}\right) \quad (1)$$

which uses the extinction coefficient of NADH ($6.22\times10^3\ M^{-1}\ cm^{-1}$), the rate of change of absorbance at 340 nm per minute (ΔOD_{340}), and accounts for the four NADH molecules oxidized per RuBP carboxylated by Rubisco in the coupled assay (Supplementary Fig. S1). Substrate-saturated Rubisco carboxylase activity in the same leaf soluble protein was measured by $^{14}CO_2$ fixation assays as described (Sharwood *et al.*, 2008). The carboxylation turnover rate (k_{cat}^c) was determined from the Rubisco activity measured by either the

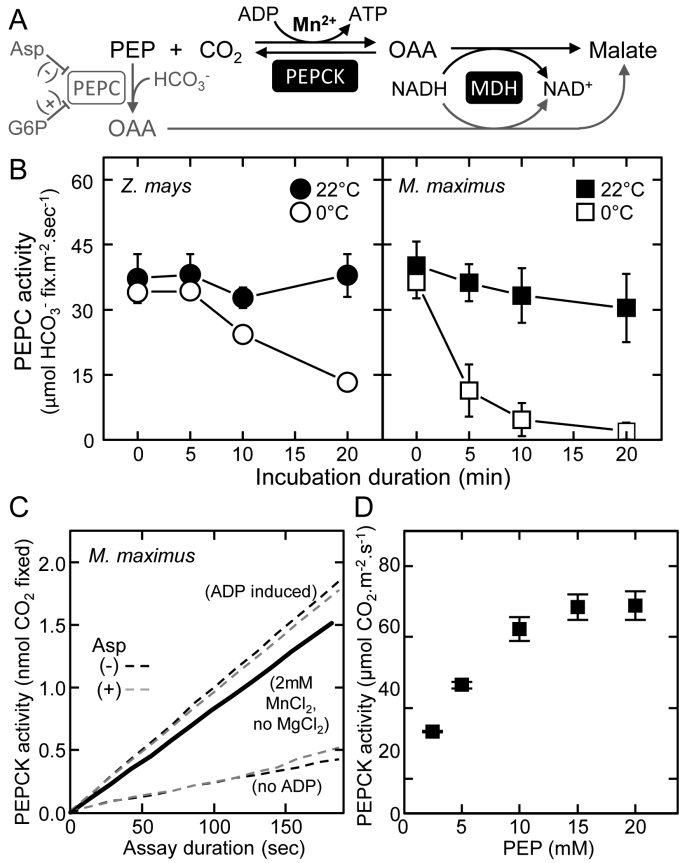

Fig. 2. Optimizing the measurement of PEPC and PEPCK activities in leaf extract. (A) Summarizing the commonality of the malate dehydrogenase- (MDH) coupled, NADH oxidation-linked assay to quantify the carboxylation of phosphoenolpyruvate (PEP) into oxaloacetate (OAA) by PEP carboxykinase (PEPCK; in black) and PEP carboxylase (PEPC; in gray), an enzyme inhibited (–) by aspartate (Asp; Huber and Edwards, 1975) and activated (+) by glucose-6-phosphate (G6P). (B) Effect of storage temperature (room temperature, 22 °C, or ice, 0 °C) and time on PEPC activity in the soluble protein from young leaves from mature *Z. mays* and *M. maximus* plants (n=3 biological replicates ±SD; see leaves m3b and c3b in Fig. 5A for examples). (C) Representative assay of PEP carboxylation by PEPCK measured in leaf soluble protein extract using the no $MgCl_2$ method of Sharwood *et al.* (2014) (black line) and the modified ADP method of this study in assays with (gray dashed lines) or without (black dashed lines) 5 mM aspartate (a PEPC inhibitor, A). (D) Response of PEPCK activity to [PEP] in *M. maximus* leaf soluble protein. To prevent PEPC interference ensure: 1) No $MgCl_2$ in assay and extraction buffers, 2) $MnCl_2$ up to 5mM in extraction and assay buffers, 3) pH of extraction and assay buffers <7.0, 4) No glucose-6-phosphate, and 5) include aspartate in assay buffer.

NADH-coupled enzyme assay or the $^{14}CO_2$ fixation assay divided by the Rubisco active site content in the assay as quantified by [^{14}C] CABP binding (Ruuska *et al.*, 1998). Time course measurements of Rubisco activity over 30 min at 25 °C were undertaken to confirm the functional integrity of Rubisco in the leaf protein extracts.

Rubisco activase purification and assay

Tobacco RCA was expressed and purified from *Escherichia coli* as described (Baker *et al.*, 2005). Two-stage assays similar to that described by Barta *et al.* (2011) were used to assess if sugar-phosphate Rubisco inhibition in tobacco leaf protein extracts influenced measurements of total Rubisco activity. In the first assay stage, 50 µl of leaf extract was incubated in a 0.5 ml final volume with 80 µg ml^{-1} RCA (or BSA in the RCA-free controls) for 2 min at 25 °C in ATPase assay buffer [100 mM EPPS, pH 8.0, 20 mM KCl, 5 mM $MgCl_2$, 6% (w/v) polyethylene glycol (PEG) (mol. wt 3350 Da)], 2 mM PEP, 0.2 mM NADH, 2 mM ATP, 1% (v/v) of a pyruvate kinase/lactate dehydrogenase mixture (PK, 745 U ml^{-1}; LDH, 906 U ml^{-1}, Sigma-Aldrich). In the second assay stage, 100 µl of the RCA leaf or BSA leaf protein reactions were added to the NADH-linked Rubisco assays and the total activities compared. Control assays examining tobacco RCA activation of purified tobacco Rubisco ER complexes are described in Supplementary Fig. S2.

Statistical analysis

Statistical analysis was carried out using one- or two-way ANOVA (Statistica, StatSoft Inc. OK, USA). Means were grouped using a post-hoc Tukey test.

Results and Discussion

Optimizing the assay of PEPC and PEPCK activities in total soluble leaf protein

Measuring PEPC and PEPCK activities separately in soluble leaf protein extracts using NADH-linked spectrophotometric assays is complicated by their common requirement for substrate PEP (Fig. 2A) particularly in assays containing Mg^{2+} and Mn^{2+} at physiological concentrations (Muhaidat and McKown, 2013). Determining maximal PEPCK activity in soluble leaf protein extracts is typically achieved by assaying the decarboxylation reaction of PEPCK, requiring purified protein free of other C_4 enzymes such as PEPC (Ashton *et al.*, 1990; Chen *et al.*, 2002). In contrast, measures of PEPC rates free of PEPCK activity can easily be made by omission of ADP from the assay (Fig. 2A). As *in vitro* measures of PEPC are sensitive to low temperature storage (Hatch and Oliver, 1978), we examined the PEPC activity in soluble leaf protein from *Z. mays* and *M. maximus* stored either at room temperature (22 °C) or on ice (0 °C) (Fig. 2B). When incubated at 22 °C for 20 min, there was little or no loss of PEPC activity evident in replica leaf samples from either *M. maximus* or *Z. mays.* In contrast, storage of the leaf protein extracts on ice significantly reduced PEPC activities (measured at 25 °C), particularly in *M. maximus* where >65% of PEPC activity was lost after 5 min at 0 °C (Fig. 2B). As a result of its sensitivity to low temperature, all assays of PEPC activity were performed on rapidly extracted (homogenized in <0.5 min and centrifuged for 0.5 min at 4 °C) leaf soluble protein without storage on ice.

In C_4 plants with phosphoenolpyruvate carboxykinase (PCK) physiology (e.g. *M. maximus*), PEPCK is the dominant decarboxylase enzyme that utilizes ATP hydrolysis during its reversible decarboxylation of OAA (Fig. 2A). In contrast to the alkali pH 8 preference of PEPC (Greenway *et al.*, 1978), the activity of PEPCK is optimal at pH 7 and 80% lower at pH 8.0 (Ray and Black, 1976; Pierre *et al.*, 2004). To minimize, possibly preclude, PEPC activity, the extraction and measurement of PEPCK carboxylase activity was undertaken at pH 7.0 with Mg^{2+} (required for PEPC activity) omitted and replaced with 2 mM Mn^{2+}, a PEPCK cofactor (Fig. 2A). Under these conditions, stable rates of PEPCK were obtained in assays initiated by the addition of PEP (solid line, Fig. 2C) (Sharwood *et al.*, 2014).

Alternative PEPCK analyses were undertaken where the assays were initiated with ADP, not PEP (Fig. 2C, black dashed line). Omission of ADP in control assays produced background rates of apparent PEPC activity (Fig. 2C, lower black dashed line); however, the addition of 5 mM aspartate (Fig. 2C, grey dashed line) or 5 mM glucose-6-phosphate (and $MgCl_2$) which inhibit and stimulate PEPC activity, respectively (Fig. 2A), had a negligible effect on the measured activities. This suggests that the background 'no ADP' PEP carboxylase activities observed arise from PEPCK activity that is utilizing residual ADP in the soluble protein extract. Consequently, we propose that extracting leaf protein in pH 7.0 buffer with no $MgCl_2$ and assaying in an $MnCl_2$-containing buffer at the same pH is sufficient to measure PEPCK activity with little or no contaminating PEPC activity.

Assays containing 2.5–25 mM PEP were used to determine that a saturating concentration of 15 mM PEP was required for maximal PEPCK activity in soluble leaf protein from 1.3 mm^2 of *M. maximus* leaf tissue (Fig. 2D). This saturating PEP concentration is 7-fold higher than the K_m for PEP measured for *M. maximus* PEPCK (Chen *et al.*, 2002) and was the concentration used in all subsequent PEPCK assays.

Measuring Rubisco carbamylation status

The carboxylase-limiting component of the C_3 photosynthesis models stemming from those derived by Farquhar *et al.* (1980) are typically used to derive estimates of $V_{c,max}$ [in units of μmol CO_2 fixed m^{-2} s^{-1}, that equate to the product of Rubisco sites (μmol CO_2 fixed m^2) and k_{cat}^c (s^{-1})]. This measure is extrapolated from the response of the CO_2 assimilation rate (A) with increasing CO_2 measured by leaf gas exchange, and relies heavily on the temperature response measurements of k_{cat}^c, K_c, the K_m for O_2 (K_o), and CO_2/O_2 specificity ($S_{c/o}$) made for tobacco Rubisco (Sharkey *et al.*, 2007). The universal suitability of these parameters is now in question given the substantial variation observed in the temperature response of these parameters among plant Rubiscos (Walker *et al.*, 2013; Boyd *et al.*, 2015; Perdomo *et al.*, 2015). Moreover, differences in $V_{c,max}$ are primarily attributed to variations in Rubisco content and generally overlook differences in the activation status of Rubisco *in vivo*, despite its critical influence on estimates of $V_{c,max}$ and *in vivo* determined k_{cat}^c (Bernacchi *et al.*, 2001; Salvucci and Crafts-Brandner, 2004).

As indicated in Fig. 1, within an illuminated leaf chloroplast the catalytic sites of Rubisco (shown as E) are primarily CO_2–Mg^{2+} activated (ECM) and capable of RuBP catalysis. Binding of inhibitory XuBP or, in darkened leaves, CA1P to ECM produces catalytically inactive ECMI complexes whose activation involves RCA-catalysed dissociation of the sugar-phosphate ligands which are then degraded by substrate-specific enzymes (Jordan and Chollet, 1983; Gutteridge *et al.*, 1986; Edmondson *et al.*, 1990; Bracher *et al.*, 2015). Thus the most abundant form of Rubisco inhibition in illuminated chloroplasts is probably the binding of RuBP to non-carbamylated Rubisco (ER) that renders the catalytic site inactive (Jordan and Chollet, 1983).

The NADH-linked spectrophotometric and $^{14}CO_2$ fixation *in vitro* assays typically used to measure Rubisco activation status involve three stages (Fig. 1). The first stage involves the rapid measure of Rubisco activity in rapidly extracted soluble leaf protein. This measures the 'initial' Rubisco activity. Saturating amounts of RuBP are included to prevent ECM formation from the ER complexes and ensure that the assays are not RuBP limited (Laing and Christeller, 1976). Replica samples of the leaf protein extracts are then allowed to activate fully by incubating in buffer lacking RuBP but containing saturating CO_2 and Mg^{2+}. During the second stage, the inconsequential RuBP levels in the extract enable its dissociation from the ER complexes to allow ECM formation. The third stage measures the 'total' Rubisco activity rate. In samples from darkened or stressed leaves, the formation of ECMI complexes can cause significant underestimation of the 'total' activities (Parry *et al.*, 1997, 2002; Carmo-Silva *et al.*, 2010) a consideration we sought to avoid in this study by sampling healthy, naturally illuminated glasshouse-grown plant material 6–7 h into the photoperiod.

Optimizing leaf protein extraction for measuring Rubisco activation status

Analyses undertaken using tobacco leaves highlighted the requirement for speed and inclusion of ~5 mM Mg^{2+} during leaf protein extraction for accurate measurements of initial Rubisco activity (Fig. 3A). As shown in Fig. 1, formation of ECM is initiated by the slow and reversible carbamylation of Lys201 in the catalytic site of E followed by the rapid binding of Mg^{2+}. To avoid Rubisco carbamylation occurring during extraction, the leaf soluble protein is extracted in N_2-sparged (i.e. CO_2-free) buffer. It was hypothesized that the exclusion of $MgCl_2$ during extraction would undesirably produce EC complexes from which the activating CO_2 would dissociate to form inactive E. Indeed, the omission of $MgCl_2$ in the CO_2-free extraction buffer led to significantly lower measurements of initial Rubisco activity (70% of maximum activity) after just 0.5 min relative to those extracted with 2–10 mM $MgCl_2$ (82–85% of maximum activity; Fig. 3A). Extending the extraction (centrifugation) period to 5 min reduced all initial Rubisco activity measurements, more so in those extracted without $MgCl_2$ (35% of maximum activity) compared with those extracted with $MgCl_2$ (55–60% of maximum activity). In all treatments, very similar total activity rates were attained, indicating that the varying extraction conditions did not compromise Rubisco integrity (Fig. 3A, circles). These findings caution against the omission of $MgCl_2$ when assaying for initial activities. Furthermore, potential inaccuracies are incurred with extended centrifugation times of >0.5–1 min following extraction, emphasizing the need for rapid leaf protein extraction and assay.

The importance of using purified RuBP

Using pure RuBP devoid of inhibitory impurities such as PDBP is critical for accurately measuring Rubisco catalysis *in vitro* (Kane *et al.*, 1998; Andralojc *et al.*, 2012). As observed by Scales *et al.* (2014), by using pure RuBP the measured rates of initial and total activity remain relatively linear over a 4 min assay period (Fig. 3B). This (i) indicates that insignificant levels

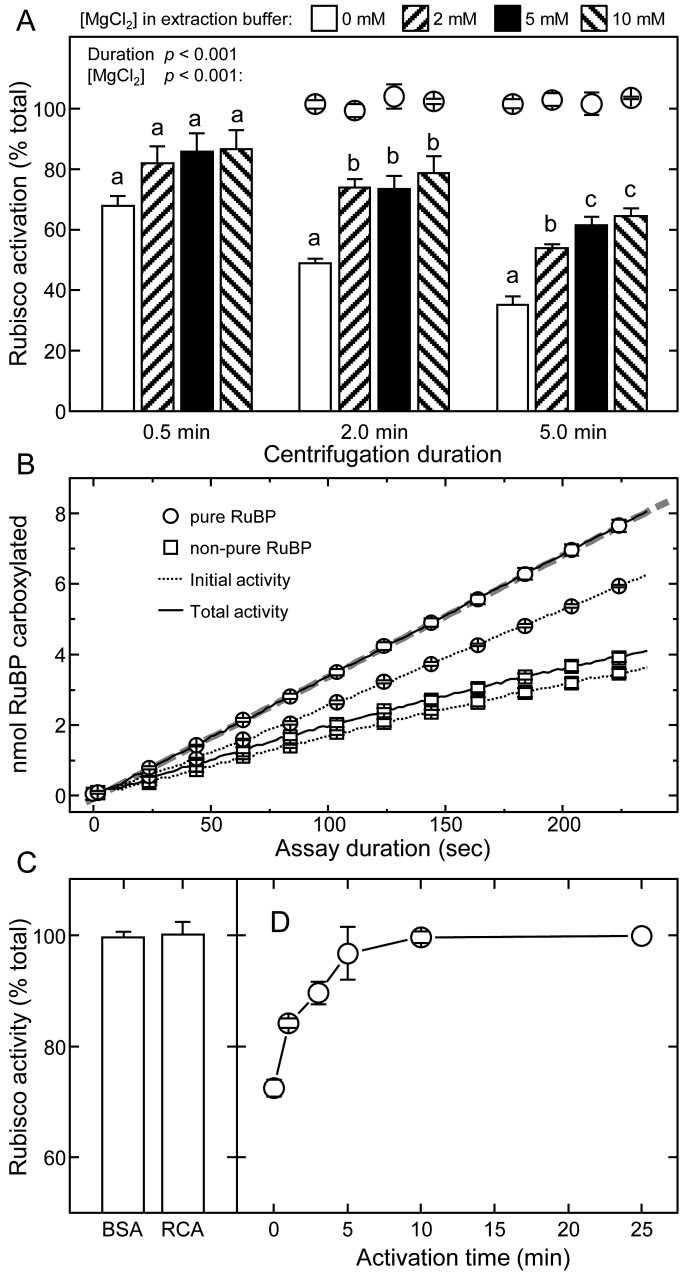

Fig. 3. Evaluating the experimental methodology for measuring leaf Rubisco activation status. (A) Appraising how $MgCl_2$ inclusion and quickness of soluble leaf protein extraction influences Rubisco activation quantification. NADH-linked assays were performed on N_2-frozen replica (n=5) tobacco leaf discs (0.5 cm^2) taken from a young, nearly fully expanded upper canopy leaf (15 cm in diameter) and stored at –80 °C for up to 3 months without effect on recoverable activity. Circles indicate the total activities measured after 10 min activation relative to the 0.5 min centrifuged sample (B) Representative NADH-linked spectrophotometric measures of initial (dashed lines) and total (solid lines) Rubisco activities made using low purity commercial RuBP (squares) or that purified according to Kane *et al.* (1998) (circles). Rates correspond to protein from 0.9 mm^2 of leaf with a Rubisco active site concentration in each assay of ~34.4 nM (i.e. a k_{cat} of 2.2 s^{-1}). (C) Incubation of leaf protein extract for 2 min at 25 °C with 80 μg ml^{-1} of either BSA or purified tobacco Rubisco activase (RCA) had no effect on the measured rates of fully activated Rubisco, while the same treatment re-activated >80% of inhibited ER complexes formed using a comparable concentration of purified tobacco Rubisco (Supplementary Fig. S2). (D) Change in the activity status of Rubisco in tobacco soluble protein activated at 25 °C for up to 25 min. Data in (C) and (D) are the averages (±SE) from analyses with three separate leaf samples expressed as a percentage of the total activities measured after 10 min (C) and 25 min (D) activation. For (A), the significance level (P) for the [$MgCl_2$] and centrifugation duration factors are shown. Letters indicate the ranking (lowest=a) of means within each centrifugation duration using a post-hoc Tukey test. Values followed by the same letter are not significantly different at the 5% level (P>0.05).

of the catalytic misfire products XuBP or PDBP are produced over the assay period; (ii) indicates that Rubisco activity in the assay is stable; and (iii) confirms the observations of Laing and Christeller (1976) that inclusion of saturating RuBP levels (0.2–0.4 mM) in the 'initial' assays prevents Rubisco activation. In contrast, Rubisco activities measured in the same extracts using a commercial source of non-pure RuBP (Fig. 3B, squares) declined rapidly, presumably due to PDBP contamination (Andralojc *et al.*, 2012). The use of non-pure RuBP further compromised the quantification of k_{cat}^c (2.2 s^{-1} with pure RuBP versus 1.3 s^{-1} with non-pure RuBP) and the calculated activation status of Rubisco (75 ± 2% with pure RuBP versus 83 ± 3% with non-pure RuBP). Use of non-pure RuBP should therefore be avoided in order to avoid underestimating the carbamylation status (Rowland-Bamford *et al.*, 1991; Anwaruzzaman *et al.*, 1996; Ruuska *et al.*, 2004; Sulpice *et al.*, 2007) and activity (Rintamäki *et al.*, 1988; Uemura *et al.*, 2000) of Rubisco.

Insignificant levels of ECMI complexes accumulate in illuminated, non-stressed leaves

The k_{cat}^c value of 2.2 s^{-1} was reproducibly quantified for tobacco Rubisco using the NADH-coupled assay. This is ~30% lower than those typically measured by $^{14}CO_2$ fixation assays (Sharwood *et al.*, 2008; Whitney *et al.*, 2011). Incubation of the leaf protein extracts with purified tobacco RCA or BSA (control) showed no difference in the measured total Rubisco activities (Fig. 3C). In corresponding control assays, the RCA treatment was able to reactivate ER inhibited Rubisco fully over 10 min (Supplementary Fig. S2). This indicates that the lower k_{cat}^c was not due to residual ECMI complexes in the leaf protein extract. To confirm this, the same tobacco soluble leaf protein was used to quantify k_{cat}^c by the $^{14}CO_2$ assay method of Sharwood *et al.* (2008). As indicated in Table 1, the expected k_{cat}^c of 3.1 s^{-1} for tobacco Rubisco was obtained by the $^{14}CO_2$ assay. This finding questions the accuracy of the NADH-coupled assay for quantifying Rubisco carboxylase activity, a deficiency also evident in the comparative measurements made by Lilley and Walker (1974). Indeed, published k_{cat}^c values determined by the NADH-coupled assay for cyanobacteria (Emlyn-Jones *et al.*, 2006) and plant (Pearce and Andrews, 2003) Rubisco are also 20–25% lower than those measured by $^{14}CO_2$ fixation (Whitney *et al.*, 1999; Mueller-Cajar and Whitney, 2008). To ensure that the differences were not due to components in the leaf extracts interfering with the coupling enzymes, comparative assays were undertaken in triplicate (technical repeats) using tobacco Rubisco purified by ion exchange chromatography (see the legend to Supplementary Fig. S2). Again, the k_{cat}^c values determined by the NADH-coupled assay (1.9 ± 0.2 s^{-1}) were 30% lower than that quantified by $^{14}CO_2$ fixation assays

Table 1. *Comparative values of Rubisco k_{cat}^c at 25 °C quantified by the NADH-linked and $^{14}CO_2$ fixation assays*

Plant species	Photosynthetic biochemistry	k_{cat}^c (±SE s^{-1})				Significance (*P*)
		NADH-linked assay		$^{14}CO_2$ assay		
Tobacco	C_3	2.15 ± 0.02 b	*n*=24	3.07 ± 0.06 b	*n*=23	<0.001
P. bisulcatum	C_3	1.79 ± 0.03 a	*n*=22	2.72 ± 0.11 a	*n*=7	<0.001
M. maximus	C_4-PCK	3.85 ± 0.09 e	*n*=9	5.17 ± 0.17 d	*n*=10	<0.001
T. aestivum	C_3	2.70 ± 0.06 c	*n*=9	3.59 ± 0.04 c	*n*=6	<0.001
Z. mays	C_4-NADP ME	3.70 ± 0.10 d	*n*=9	5.46 ± 0.10 d	*n*=6	<0.001

Values (means ±SE) obtained using NADH-linked and $^{14}CO_2$ assays were compared by one-way ANOVA, and the significance level (*P*) is shown. Species' means obtained by each of the assay types were ranked separately using a post-hoc Tukey test. Values followed by the same letter are not significantly different at the 5% level (*P*>0.05).
n=number of leaf protein samples (biological replicates) analyzed.

($2.7 \pm 0.1\ s^{-1}$). This suggests that substrate limitations for one or more of the enzymes in the NADH-linked assay limit its potential for accurately quantifying k_{cat}^c, possibly the rate of 3-PGA reduction (Lilley and Walker, 1974).

The need for measuring Rubisco activation rate and stability over time

Given that the NADH-coupled assay allows for the continued 'real-time' monitoring of both initial and total Rubisco activity (Fig. 3B), it was used to examine the activation rate and stability of Rubisco activity at 25 °C in the soluble protein of leaves from the C_3 species *P. bisulcatum* and *T. aestivum* (wheat), and the C_4 species *M. maximus* and *Z. mays.* Linear rates of initial and total Rubisco activities were reproducibly found for each sample (Fig. 4A), with the rates of NADH oxidation significantly lower in the C_4 samples due to their low Rubisco contents. As shown in Fig. 4A, the k_{cat}^c for both C_4 Rubiscos were seen to be higher than those of their C_3 counterparts when the activities were corrected for Rubisco content (quantified by [^{14}C]CABP binding).

Like tobacco, full activation of Rubisco in the soluble protein extracted from wheat and *P. bisulcatum* required 10 min incubation at 25 °C (Fig. 4B, circles). In contrast, full activation of Rubisco in the *M. maximus* and *Z. mays* leaf protein required only 3–5 min (Fig. 4B). Whether the faster rate of Rubisco activation in both C_4 species arises from a lower RuBP binding affinity remains a subject for future investigation. Nevertheless, variation in the time needed to activate Rubisco fully in leaf protein extracts questions whether shorter incubation times (e.g. 3 min) are sufficient to evaluate Rubisco activation status accurately and extrapolate ECMI levels (Parry *et al.*, 1997, 2002; Carmo-Silva *et al.*, 2010; Galmes *et al.*, 2011; Scales *et al.*, 2014).

The k_{cat}^c of C_4 plant Rubisco exceeds that of C_3 Rubisco

The k_{cat}^c values of Rubisco from the C_4 species examined in this study were significantly faster relative to that of each C_3 plant Rubisco (Table 1). Notably the NADH-coupled assay measures of k_{cat}^c were again 30–35% lower than corresponding k_{cat}^c measurements made using $^{14}CO_2$ fixation assays (Table 1). Statistical ranking of the catalytic speed indicated

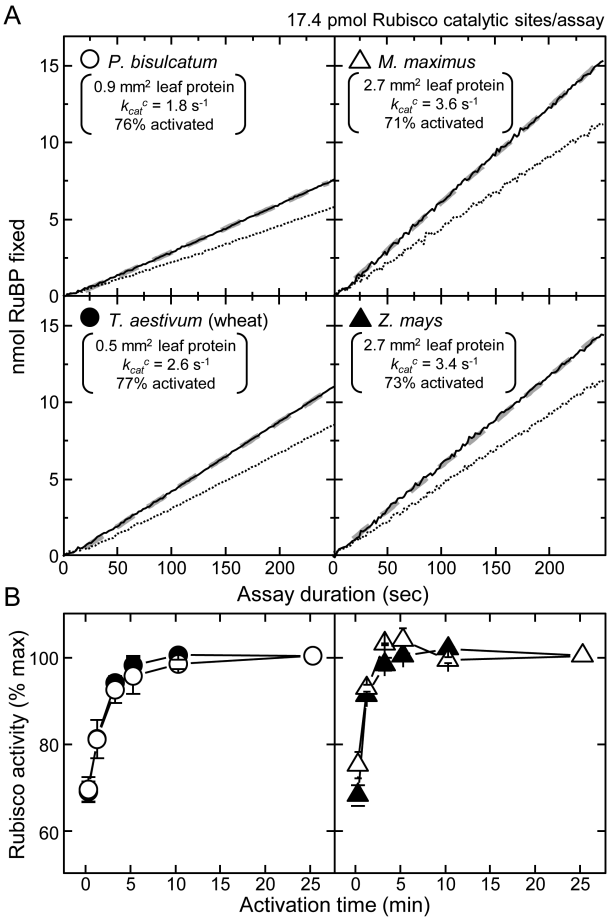

Fig. 4. Variations in Rubisco content and activation status during leaf ontogeny can account for variations in the *in vivo* estimates of V_c^{max}. (A) Representative NADH-linked assay data showing the linear RuBP carboxylation rates in assays of initial (dashed lines) and total (solid lines, after 10–15 min activation) Rubsico activities at 25 °C using soluble leaf protein from both C_3 (*P. bisulcatum*, *T. aestivum*) and C_4 (*M. maximus*, *Z. mays*) monocotyledon species. Shown are details of the calculated Rubisco activation status (% of maximum), the derived carboxylation rates (k_{cat}^c, quantified from the slope of the fitted linear regression, gray dashed line, divided by Rubisco content quantified by [^{14}C]CABP binding) and the area of leaf protein required to attain the 17.4 pmol Rubsico catalytic sites used to normalize the plotted data to highlight the variations in k_{cat}^c between each species (see also Table 1). (B) Response of Rubisco activation and activity in the soluble leaf protein of each species following incubation at 25 °C. Shown is the average (±SE) of analyses from three separate leaf samples for each species expressed as a percentage of the maximum activities measured after 25 min activation.

that the C_3 Rubisco from *P. bisulcatum* is slower than that of tobacco, with wheat outperforming both ($P<0.001$). In contrast to its ancestral *P. bisulcatum* Rubisco, the k_{cat}^c for *M. maximus* Rubisco is ~2-fold higher but similar to the k_{cat}^c of maize Rubisco despite originating from different biochemical subtypes and evolutionary origins (Table 1).

How do PEPC, Rubisco content, and activation status vary with leaf age?

Rubisco comprises a significant but variable N investment in plant leaves. In tobacco, wheat, and rice, Rubisco comprises 20–30% of the leaf N, which is equivalent to 30–60% of the leaf soluble protein (Evans, 1989; Makino *et al.*, 2003; Whitney *et al.*, 2011), while in C_4 plants it is 5–10% (Ghannoum *et al.*, 2005). The lower Rubisco requirement of C_4 plants stems from their CCM that enables them to operate under near saturating CO_2 concentration, which has facilitated the evolution of increased Rubisco k_{cat}^c (Ghannoum *et al.*, 2005). Consistent with these findings, the variation in Rubisco content with leaf ontogeny and at different locations in the canopy of *M. maximus* and maize (Fig. 5A) was 3- to 25-fold lower than that measured in C_3 species (tobacco, *P. bisulcatum*, and wheat, Fig. 5B). Among the C_3 plants, significantly higher levels of Rubisco were measured in wheat relative to tobacco and *P. bisulcatum*, with the latter grass showing the greatest variation in Rubisco content (per leaf area) in the leaves from juvenile and mature plants.

The variation in Rubisco with leaf ontogeny evident in both C_4 species was somewhat mirrored by differences in their PEPC activities (Fig. 5B), resulting in similar PEPC:Rubisco activity ratios of ~3.9–5.7 in *M. maximus* that were more varied in maize (4.2–7.9 in juvenile plant leaves and 8.5–9.3 in the young leaves of exponentially growing plants; Fig. 5C). This ratio is typically used as an indication of the CO_2 supply to the CCM in C_4 plants and is normally in balance to minimize leakage of fixed CO_2 (von Caemmerer, 2000; von Caemmerer *et al.*, 2014). In both *M. maximus* and *Z. mays*, the PEPC:Rubisco ratio tended to increase during ontogeny, in particular when the ratio is adjusted with regard to differences in Rubisco activation status (Fig. 5C). The higher Rubisco:PEPC ratio in mature *Z. mays* leaves relative to *M. maximus* may arise from their varying C_4 biochemistry and/or evolutionary origin, a consideration beyond the objectives of this study.

Despite being produced in lower abundance, the activation status of C_4 Rubisco was similar or lower than that measured in the C_3 species. Similarly, low levels of Rubisco activation (~45–55%) have been measured in other C_4 species (von Caemmerer *et al.*, 2005; Carmo-Silva *et al.*, 2010) that correlate with those measured in mature *M. maximus* and *Z. mays* leaves (Fig. 5D). Higher Rubisco activation levels (~70–80%) were measured in the juvenile C_4 plant leaves. These levels matched those measured in tobacco and *P. bisulcatum*, where little variation in Rubisco activation status was found among the leaves sampled. In contrast, significant variation in Rubisco activation status was observed among the upper wheat panicle leaves, where Rubisco activation was significantly lower than those sampled from juvenile plants (Fig. 5D).

The level of variation in Rubisco content and activation status with leaf ontogeny identified within this explorative study using plants grown under non-stress conditions emphasizes the importance of determining these parameters to compare meaningfully values of $V_{c,max}$ derived by extrapolation from leaf gas exchange (A–C_i curves) for different biological samples. As demonstrated by Whitney and Sharwood (2014), quantifying the leaf Rubisco content is best achieved using the [^{14}C]CABP binding methods as densitometry methods following PAGE separation of Rubisco are highly imprecise, unless appropriately calibrated. Accurate quantification of Rubisco site content in the *in vitro* assays of Rubisco activity are also critical for quantifying k_{cat}^c. This parameter also provides a number of quality checks as reduced measures of k_{cat}^c provide a useful indicator of reduced leaf sample viability (as found if ultra-cold temperatures are not maintained during transfer and storage at –80 °C) and incomplete activation (e.g. insufficient activation time and/or presence of significant levels of ECMI complexes in the sample).

Variation in NADP-ME and PEPCK activities in Z. mays *and* M. maximus.

Different aged leaves sampled from mature *M. maximus* and *Z. mays* plants were analysed for maximal NADP-ME and PEPCK activities (Fig. 6). Higher PEPCK activities were measured in the younger leaves from both species, with as much as 2-fold higher activity measured in the *Z. mays* samples. Conversely, NADP-ME levels were characteristically >10-fold higher in *Z. mays*, consistent with its C_4-NADP-ME photosynthetic biochemistry. While the low NADP-ME activity in *M. maximum* probably arose from an anaplerotic reaction, the significance of the PEPCK activity in *Z. mays* is not yet fully understood. Prior analysis of *Z. mays* exposed to salinity stress and shade treatments showed that there is plasticity in PEPCK contents and activity (Sharwood *et al.*, 2014). This suggests that the PEPCK decarboxylation pathway may serve a role in responding to stressful environmental cues (Bellasio and Griffiths, 2014).

Conclusion

In this study, we demonstrate the need for carefully considering the experimental requirements needed to measure accurately, and reproducibly, the activity of key carboxylase and decarboxylase enzymes that are commonly used to evaluate physiological and biochemical parameters between plant samples. Of particular relevance to C_3 and C_4 photosynthetic modelling studies is how Rubisco content and activation can vary significantly with leaf ontogeny, in particular in C_4 plants where Rubisco activation appears characteristically low. Here we show that full Rubisco activity is recoverable *in vitro* without the need for RCA when extracted with no RuBP. We therefore propose that Rubisco inactivation in the chloroplasts of non-stressed, illuminated leaves is primarily attributable to ER complex formation. Removing Rubisco inhibitors using Na_2SO_4 and PEG treatments (Parry *et al.*, 1997, 2002; Carmo-Silva *et al.*, 2010; Galmes *et al.*, 2011; Scales *et al.*,

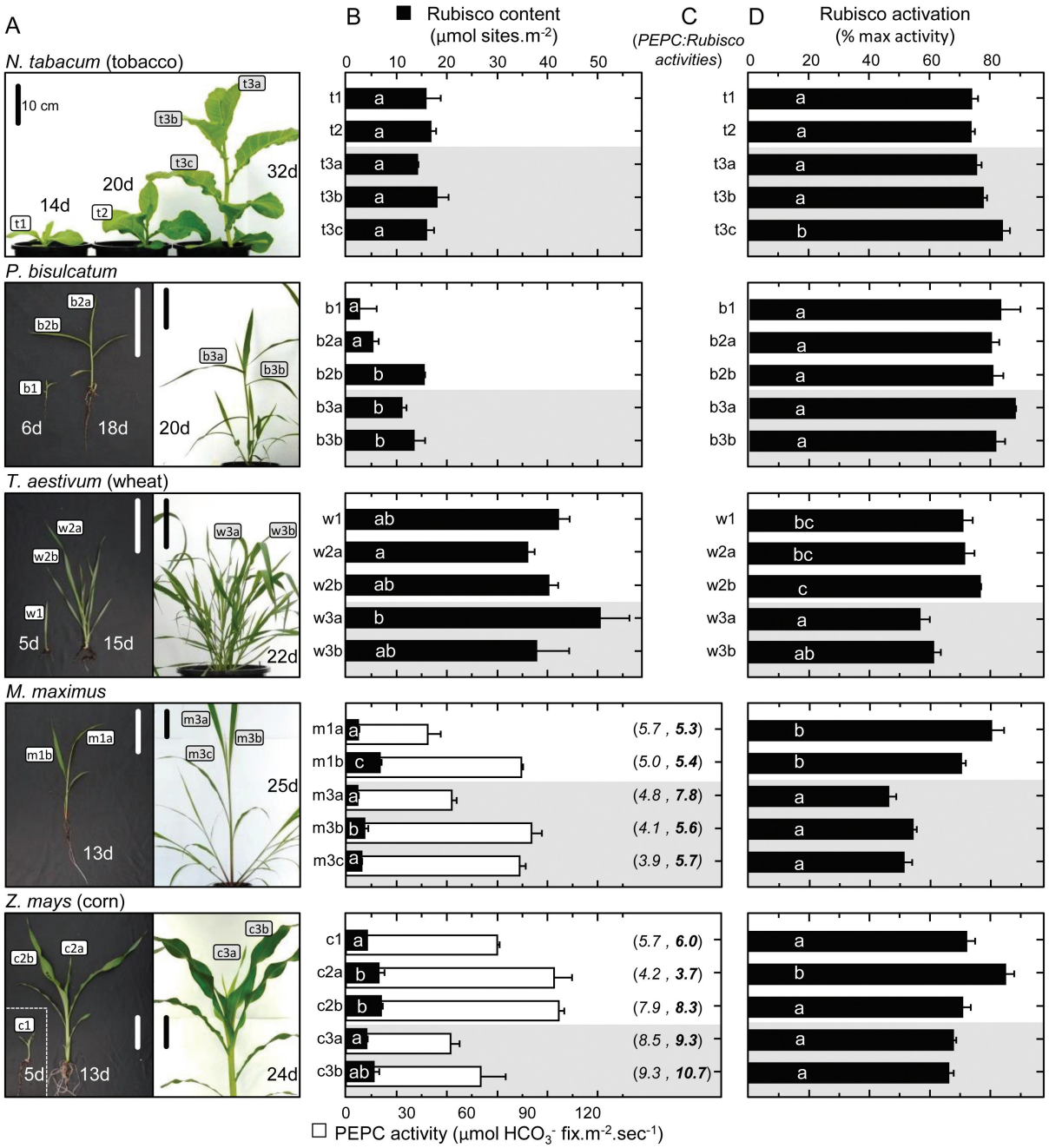

Fig. 5. Variation in PEPC activity, Rubisco content, and Rubisco activation status with leaf ontogeny and development in C_3 and C_4 plants. (A) Pictures showing the leaves at differing stages of ontogeny and plant development (as labeled) that were analyzed for (B) Rubisco content (black bars, determined by [^{14}C]CABP binding) and PEPC activity (white bars). (C) For both C_4 species, the corresponding PEPC:Rubisco activity ratios are shown in parenthess; the first value is determined from the rates measured using the NADH-linked assays (in italics) and the second value (in bold) takes into account the higher Rubisco k_{cat}^c values quantified using $^{14}CO_2$ assays (Table 1) and (D) the activation status of Rubisco in each leaf analyzed. The age of each plant (days, d) post-cotyledon emergence is indicated with the scale bar=10 cm. All data are averages (±SD) of n=3 leaf discs taken from each leaf (or for the juvenile samples b1, c1, and w1, from replica plantlets). Regions shaded gray in (B) and (D) indicates data for leaves sampled from more mature plants. For (B) and (D), letters indicate the ranking (lowest=a) of means within each species using a post-hoc Tukey test. Values followed by the same letter are not significantly different at the 5% level (P>0.05). The levels of Rubisco measured correlate with those previously measured in the leaves of tobacco (Whitney *et al.*, 2011), *P. bisulcatum* (Pinto *et al.*, 2014), *M. maximus* (Pinto *et al.*, 2016), and maize (Sharwood *et al.*, 2014).

2014) that can potentially harm recoverable activity might therefore be unnecessary using the *in vitro* assay conditions described in this study.

As summarized in Supplementary Fig. S3, we identified the core requirements for measuring Rubisco activation status (fast extraction, include ~5 mM $MgCl_2$, use pure RuBP, activate for 10 min), PEPC (pH 8, 22 °C post-extraction), PEPCK (pH 7, >2 mM Mn^{2+} no Mg^{2+}, 15 mM PEP), and NADP-ME activities using NADH-linked assays. We highlight how an unresolved limitation in the NADH linked assay underestimates Rubisco k_{cat}^c by >20%. We also emphasize the advantage of quantifying Rubisco by [^{14}C]CABP binding

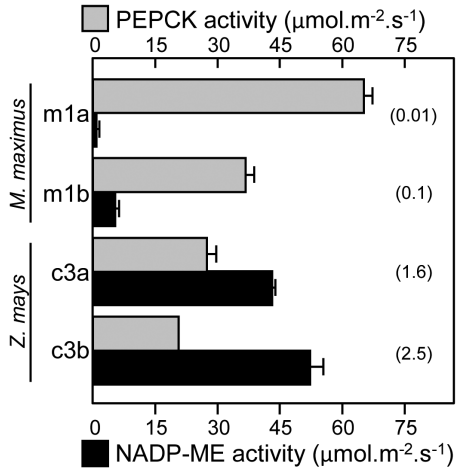

Fig. 6. Maximal activity of the decarboxylases in C_4 grasses. Comparison of PEPCK (gray) and NADP-ME (black) activities in differing aged *Z. mays* and *M. maximus* leaves (n=3, ± SE). The leaves analyzed are shown in Fig. 4A. The PEPCK:NADP-ME ratio activities are indicated in parentheses.

to normalize Rubisco activities per active site (i.e. k_{cat}^{c}) as it serves as a quality control indicator of sample integrity and full Rubisco activation. Understandably, the assay and extraction conditions used in this study probably need optimization for other plant samples where additives and conditions (pH, temperature) are required to sustain, or promote, enzyme activities (Supplementary Fig. S3). As shown here by the differing assay requirements of PEPC and PEPCK, this optimization should also assess the compatibility of additives on the activity of each enzyme measured.

Supplementary data

Supplementary data are available at *JXB* online.

Table S1. Details for the preparation and storage of coupling enzymes used in the NADH-linked spectrophotometric assay of Rubisco activity.

Figure S1. Overview of the NADH-linked enzyme-coupled spectrophotometric assay for measuring Rubisco activity.

Figure S2. Time-dependent activation in vitro of inhibited tobacco Rubisco–RuBP (ER) complexes by RCA.

Figure S3. Core requirements for measuring Rubisco activation status, PEPC, PEPCK, and NADP-ME activities.

Acknowledgements

This research was funded by the Australian Research Council which spans the following grants: DE130101760 (RES), DP120101603 (OG, SMW), and CE140100015 (OG, SMW).

References

Andersson I. 2008. Catalysis and regulation in Rubisco. Journal of Experimental Botany **59,** 1555–1568.

Andersson I, Backlund A. 2008. Structure and function of Rubisco. Plant Physiology and Biochemistry **46,** 275–291.

Andralojc PJ, Madgwick PJ, Tao Y, *et al*. 2012. 2-Carboxy-D-arabinitol 1-phosphate (CA1P) phosphatase: evidence for a wider role in plant Rubisco regulation. Biochemical Journal **442,** 733–742.

Andrews TJ, Whitney SM. 2003. Manipulating ribulose bisphosphate carboxylase/oxygenase in the chloroplasts of higher plants. Archives of Biochemistry and Biophysics **414,** 159–169.

Anwaruzzaman, Nakano Y, Yokota A. 1996. Different location in dark-adapted leaves of *Phaseolus vulgaris* of ribulose-1,5-bisphosphate carboxylase/oxygenase and 2-carboxyarabinitol 1-phosphate. FEBS Letters **388,** 223–227.

Ashton AR, Burnell JN, Furbank RT, Jenkins CLD, Hatch MD. 1990. Enzymes of C_4 photosynthesis. In: Lea PJ, ed. Methods in Plant Biochemistry , **Vol. 3**. London: Academic Press, 39–71.

Baker RT, Catanzariti AM, Karunasekara Y, Soboleva TA, Sharwood R, Whitney S, Board PG. 2005. Using deubiquitylating enzymes as research tools. Methods in Enzymology **398,** 540–554.

Barta C, Carmo-Silva AE, Salvucci ME. 2011. Rubisco activase activity assays. Methods in Molecular Biology **684,** 375–382.

Bauwe H, Hagemann M, Fernie AR. 2010. Photorespiration: players, partners and origin. Trends in Plant Science **15,** 330–336.

Bellasio C, Griffiths H. 2014. The operation of two decarboxylases (NADP-ME and PEPCK), transamination and partitioning of C_4 metabolic processes between mesophylll and bundle sheath cells allows light capture to be balanced for the maize C_4 pathway. Plant Physiology **164,** 466–480.

Bernacchi CJ, Singsaas EL, Pimentel C, Portis AR, Long SP. 2001. Improved temperature response functions for models of Rubisco-limited photosynthesis. Plant, Cell and Environment **24,** 253–259.

Boyd RA, Gandin A, Cousins AB. 2015. Temperature response of C_4 photosynthesis: Biochemical analysis of Rubisco, phosphoenolpyruvate carboxylase and carbonic anhydrase in *Setaria viridis*. Plant Physiology **169,** 1850–1861.

Bracher A, Sharma A, Starling-Windhof A, Hartl FU, Hayer-Hartl M. 2015. Degradation of potent Rubisco inhibitor by selective sugar phosphatase. Nature Plants **1,** 14002.

Carmo-Silva AE, Keys AJ, Andralojc PJ, Powers SJ, Arrabaca MC, Parry MA. 2010. Rubisco activities, properties, and regulation in three different C_4 grasses under drought. Journal of Experimental Botany **61,** 2355–2366.

Chen ZH, Walker RP, Acheson RM, Leegood RC. 2002. Phosphoenolpyruvate carboxykinase assayed at physiological concentrations of metal ions has a high affinity for CO_2. Plant Physiology **128,** 160–164.

Crafts-Brandner SJ, Salvucci ME. 2000. Rubisco activase constrains the photosynthetic potential of leaves at high temperature and CO_2. Proceedings of the National Academy of Sciences, USA **97,** 13430–13435.

Edmondson DL, Badger MR, Andrews TJ. 1990. Slow inactivation of ribulosebisphosphate carboxylase during catalysis is caused by accumulation of a slow, tight-binding inhibitor at the catalytic site. Plant Physiology **93,** 1390–1397.

Edwards EJ, Osborne CP, Stromberg CA ***et al***. 2010. The origins of C_4 grasslands: integrating evolutionary and ecosystem science. Science **328,** 587–591.

Emlyn-Jones D, Woodger FJ, Price GD, Whitney SM. 2006. RbcX can function as a Rubisco chaperonin, but is non-essential in *Synechococcus* PCC7942. Plant and Cell Physiology **47,** 1630–1640.

Evans JR. 1989. Photosynthesis and nitrogen relationships in leaves of C_3 plants. Oecologia **78,** 9–19.

Farquhar GD, von Caemmerer S, Berry JA. 1980. A biochemical model of photosynthetic CO_2 assimilation in leaves of C_3 species. Planta **149,** 78–90.

Furbank RT. 2011. Evolution of the C_4 photosynthetic mechanism: are there really three C_4 acid decarboxylation types? Journal of Experimental Botany **62,** 3103–3108.

Galmes J, Ribas-Carbo M, Medrano H, Flexas J. 2011. Rubisco activity in Mediterranean species is regulated by the chloroplastic CO_2 concentration under water stress. Journal of Experimental Botany **62,** 653–665.

Ghannoum O, Evans JR, Chow WS, Andrews TJ, Conroy JP, von Caemmerer S. 2005. Faster Rubisco is the key to superior nitrogen-use efficiency in NADP-malic enzyme relative to NAD-malic enzyme C_4 grasses. Plant Physiology **137,** 638–650.

Greenway H, Winter K, Luttge U. 1978. Phosphoenolpyruvate carboxylase during development of Crassulacean acid metabolism and during a diurnal cycle in *Mesembryanthemum crystallinum.* Journal of Experimental Botany **29,** 547–559.

Gutteridge S, Parry MAJ, Burton S, Keys AJ, Mudd A, Feeney J, Servaites JC, Pierce J. 1986. A nocturnal inhibitor of carboxylation in leaves. Nature **324,** 274–276.

Hatch MD. 1987. C_4 photosynthesis: a unique blend of modified biochemistry, anatomy and ultrastructure. Biochimica et Biophysica Acta **895,** 81–106.

Hatch MD, Oliver IR. 1978. Activation and inactivation of phosphoenolpyruvate carboxylase in leaf extracts from C_4 species. Australian Journal of Plant Physiology **5,** 571–580.

Jordan DB, Chollet R. 1983. Inhibition of ribulose bisphosphate carboxylase by substrate ribulose 1,5-bisphosphate. Journal of BIological Chemistry **258,** 13752–13758.

Kanai R, Edwards GE. 1999. The biochemistry of C_4 photosynthesis. In: Rowan FS, Russell KM, eds. C_4 plant biology . San Diego: Academic Press, 49–87.

Kane HJ, Wilkin JM, Portis AR, Andrews TJ. 1998. Potent inhibition of ribulose-bisphosphate carboxylase by an oxidized impurity in ribulose-1,5-bisphosphate. Plant Physiology **117,** 1059–1069.

Kim K, Portis AR. 2005. Temperature dependence of photosynthesis in Arabidopsis plants with modifications in Rubisco activase and membrane fluidity. Plant and Cell Physiology **46,** 522–530.

Koteyeva NK, Voznesenskaya EV, Edwards GE. 2015. An assessment of the capacity for phosphoenolpyruvate carboxykinase to contribute to C_4 photosynthesis. Plant Science **235,** 70–80.

Kromdijk J, Schepers HE, Albanito F, Fitton N, Carroll F, Jones MB, Finnan J, Lanigan GJ, Griffiths H. 2008. Bundle sheath leakiness and light limitation during C_4 leaf and canopy CO_2 uptake. Plant Physiology **148,** 2144–2155.

Kubien DS, Brown CM, Kane HJ. 2011. Quantifying the amount and activity of Rubisco in leaves. Methods in Molecular Biology **684,** 349–362.

Laing WA, Christeller JT. 1976. A model for the kinetics of activation and catalysis of ribulose 1,5-bisphosphate carboxylase. Biochemical Journal **159,** 563–570.

Lilley RM, Walker DA. 1974. An improved spectrophotometric assay for ribulosebisphosphate carboxylase. Biochimica et Biophysica Acta **358,** 226–229.

Long Stephen P, Marshall-Colon A, Zhu X-G. 2015. Meeting the global food demand of the future by engineering crop photosynthesis and yield potential. Cell **161,** 56–66.

Makino A, Sakuma H, Sudo E, Mae T. 2003. Differences between maize and rice in N-use efficiency for photosynthesis and protein allocation. Plant and Cell Physiology **44,** 952–956.

Moore BD, Seemann JR. 1992. Metabolism of 2'-carboxyarabinitol in leaves. Plant Physiology **99,** 1551–1555.

Mueller-Cajar O, Stotz M, Bracher A. 2014. Maintaining photosynthetic CO_2 fixation via protein remodelling: the Rubisco activases. Photosynthesis Research **119,** 191–201.

Mueller-Cajar O, Whitney SM. 2008. Evolving improved *Synechococcus* Rubisco functional expression in *Escherichia coli*. Biochemical Journal **414,** 205–214.

Muhaidat R, McKown AD. 2013. Significant involvement of PEP-CK in carbon assimilation of C_4 eudicots. Annals of Botany **111,** 577–589.

Parry MAJ, Andralojc PJ, Khan S, Lea PJ, Keys AJ. 2002. Rubisco activity: effects of drought stress. Annals of Botany **89,** 833–839.

Parry MAJ, Andralojc PJ, Parmar S, Keys AJ, Habash D, Paul MJ, Alred R, Quick WP, Servaites JC. 1997. Regulation of Rubisco by inhibitors in the light. Plant, Cell and Environment **20,** 528–534.

Parry MAJ, Andralojc PJ, Scales JC, Salvucci ME, Carmo-Silva AE, Alonso H, Whitney SM. 2013. Rubisco activity and regulation as targets for crop improvement. Journal of Experiemental Botany **64,** 717–730.

Parry MAJ, Keys AJ, Madgwick PJ, Carmo-Silva AE, Andralojc PJ. 2008. Rubisco regulation: a role for inhibitors. Journal of Experimental Botany **59,** 1569–1580.

Pearce FG. 2006. Catalytic by-product formation and ligand binding by ribulose bisphosphate carboxylases from different phylogenies. Biochemical Journal **399,** 525–534.

Pearce FG, Andrews TJ. 2003. The relationship between side reactions and slow inhibition of ribulose-bisphosphate carboxylase revealed by a loop 6 mutant of the tobacco enzyme. Journal of Biological Chemistry **278,** 32526–32536.

Pengelly JJL, Tan J, Furbank RT, von Caemmerer S. 2012. Antisense reduction of NADP-malic enzyme in *Flaveria bidenti*s reduces flow of CO_2 through the C_4 cycle. Plant Physiology **160,** 1070–1080.

Perdomo JA, Cavanagh AP, Kubien DS, Galmés J. 2015. Temperature dependence of in vitro Rubisco kinetics in species of *Flaveria* with different photosynthetic mechanisms. Photosynthesis Research **124,** 67–75.

Pierre J-N, Prieto J-L, Gadal P, Vidal J. 2004. In situ C_4 phosphoenolpyruvate carboxylase activity and kinetic properties in isolated *Digitaria sanguinalis* mesophyll cells. Photosynthesis Research **79,** 349–355.

Pinto H, Powell JR, Sharwood RE, Tissue DT, Ghannoum O. 2016. Variations in nitrogen use efficiency reflect the biochemical subtype while variations in water use efficiency reflect the evolutionary lineage of C_4 grasses at inter-glacial CO_2. Plant, Cell and Environment **39,** 514–526.

Pinto H, Sharwood RE, Tissue DT, Ghannoum O. 2014. Photosynthesis of C_3, C_3–C_4, and C_4 grasses at glacial CO_2. Journal of Experimental Botany **65,** 3669–3681.

Price GD, Pengelly JJL, Forster B, Du J, Whitney SM, von Caemmerer S, Badger MR, Howitt SM, Evans JR. 2013. The cyanobacterial CCM as a source of genes for improving photosynthetic CO_2 fixation in crop species. Journal of Experimental Botany **64,** 753–768.

Raines CA. 2003. The Calvin cycle revisited. Photosynthesis Research **75,** 1–10.

Ray TB, Black CC. 1976. Characterization of phosphoenolpyruvate carboxykinase from *Panicum maximum*. Plant Physiology **58,** 603–607.

Rintamäki E, Keys AJ, Parry MAJ. 1988. Comparison of the specific activity of ribulose-1,5-bis-phosphate carboxylase-oxygenase from some C_3 and C_4 plants. Physiologia Plantarum **74,** 326–331.

Rowland-Bamford AJ, Baker JT, Allen LH, Bowes G. 1991. Acclimation of rice to changing atmospheric carbon dioxide concentration. Plant, Cell and Environment **14,** 577–583.

Ruuska S, Andrews TJ, Badger MR, Hudson GS, Laisk A, Price GD, Caemmerer Sv. 1998. The interplay between limiting processes in C_3 photosynthesis studied by rapid-response gas exchange using transgenic tobacco impaired in photosynthesis. Functional Plant Biology **25,** 859–870.

Ruuska SA, Schwender J, Ohlrogge JB. 2004. The capacity of green oilseeds to utilize photosynthesis to drive biosynthetic processes. Plant Physiology **136,** 2700–2709.

Sage RF. 2004. The evolution of C_4 photosynthesis New Phytologist **161,** 341–370.

Sage RF, Sage TL, Kocacinar F. 2012. Photorespiration and the evolution of C_4 photosynthesis. Annual Reviews of Plant Biology **63,** 19–47.

Salvucci ME, Crafts-Brandner SJ. 2004. Inhibition of photosynthesis by heat stress: the activation state of Rubisco as a limiting factor in photosynthesis. Physiologia Plantarum **120,** 179–186.

Salvucci ME, Holbrook GP. 1989. Purification and properties of 2-carboxy-D-arabinitol 1- phosphatase. Plant Physiology **90,** 679–685.

Scales JC, Parry MAJ, Salvucci ME. 2014. A non-radioactive method for measuring Rubisco activase activity in the presence of variable ATP: ADP ratios, including modifications for measuring the activity and activation state of Rubisco. Photosynthesis Research **119,** 355–365.

Sharkey TD, Bernacchi CJ, Farquhar GD, Singsaas EL. 2007. Fitting photosynthetic carbon dioxide response curves for C_3 leaves. Plant, Cell and Environment **30,** 1035–1040.

Sharwood R, von Caemmerer S, Maliga P, Whitney S. 2008. The catalytic properties of hybrid Rubisco comprising tobacco small and sunflower large subunits mirror the kinetically equivalent source Rubiscos and can support tobacco growth. Plant Physiology **146,** 83–96.

Sharwood RE, Sonawane BV, Ghannoum O. 2014. Photosynthetic flexibility in maize exposed to salinity and shade. Journal of Experimental Botany **65,** 3715–3724.

Sharwood RE, Whitney SM. 2014. Correlating Rubisco catalytic and sequence diversity within C_3 plants with changes in atmospheric CO_2 concentrations. Plant, Cell and Environment **37,** 1981–1984.

Sulpice R, Tschoep H, Von Korf M, Bussis D, Usadel B, Hohne M, Witucka-Wall H, Altmann T, Stitt M, Gibon Y. 2007. Description and applications of a rapid and sensitive non-radioactive microplate-based assay for maximum and initial activity of D-ribulose-1,5-bisphosphate carboxylase/oxygenase. Plant Cell & Environment **30,** 1163–1175.

Uemura K, Shibata N, Anwaruzzaman, Fujiwara M, Higuchi T, Kobayashi H, Kai Y, Yokota A. 2000. The role of structural intersubunit microheterogeneity in the regulation of the activity in hysteresis of ribulose 1, 5-bisphosphate carboxylase/oxygenase. Journal of Biochemistry **128,** 591–599.

von Caemmerer S. 2000. Biochemical models of leaf photosynthesis. Melbourne: CSIRO Publishing.

von Caemmerer S, Ghannoum O, Pengelly JJL, Cousins AB. 2014. Carbon isotope discrimination as a tool to explore C_4 photosynthesis. Journal of Experimental Botany **65,** 3459–3470.

von Caemmerer S, Hendrickson L, Quinn V, Vella N, Millgate AG, Furbank RT. 2005. Reductions of Rubisco activase by antisense RNA in the C_4 plant *Flaveria bidentis* reduces Rubisco carbamylation and leaf photosynthesis. Plant Physiology **137,** 747–755.

Walker B, Ariza LS, Kaines S, Badger MR, Cousins AB. 2013. Temperature response of in vivo Rubisco kinetics and mesophyll conductance in *Arabidopsis thaliana*: comparisons to *Nicotiana tabacum*. Plant, Cell and Environment **36,** 2108–2119.

Walker RP, Chen ZH, Acheson RM, Leegood RC. 2002. Effects of phosphorylation on phosphoenolpyruvate carboxykinase from the C_4 plant Guinea grass. Plant Physiology **128,** 165–172.

Whitney SM, Baldet P, Hudson GS, Andrews TJ. 2001. Form I Rubiscos from non-green algae are expressed abundantly but not assembled in tobacco chloroplasts. The Plant Journal **26,** 535–547.

Whitney SM, Sharwood RE. 2014. Plastid transformation for Rubisco engineering and protocols for assessing expression. Methods in Molecular Biology **1132,** 245–262.

Whitney SM, Sharwood RE, Orr D, White SJ, Alonso H, Galmés J. 2011. Isoleucine 309 acts as a C_4 catalytic switch that increases ribulose-1,5-bisphosphate carboxylase/oxygenase (Rubisco) carboxylation rate in *Flaveria*. Proceedings of the National Academy of Sciences, USA **108,** 14688–14693.

Whitney SM, von Caemmerer S, Hudson GS, Andrews TJ. 1999. Directed mutation of the Rubisco large subunit of tobacco influences photorespiration and growth. Plant Physiology **121,** 579–588.